Proceedings of the Third B-J-K Symposium on Biomechanics, Healthcare and Information Science. p. 137-154 , March 16-17, 2007, Kanazawa, Japan.

SPEECH PATTERNS IN A MUSCULAR HYDROSTAT: LIP, TONGUE AND GLOSSECTOMY MOVEMENT.

Maureen Stone and Emi Z. Murano
University of Maryland Dental School
Baltimore, MD, 21201, USA

Abstract. This paper aims to use the muscular hydrostat model to explain patterns of strain and motion in soft tissue structures of the oral cavity. The lips and tongue are both muscular hydrostats in that they are composed entirely of soft tissue and moved by local deformation. Muscles are organized in orthogonal directions, which allow finely controlled and reciprocal motion. The structures also are volume preserving, so that every local compression is compensated for by an expansion. This paper presents lip data as an example muscular hydrostat structures and shows how high resolution MRI and tagged cine-MRI depict muscle anatomy and associated local strains. Normal tongue data are then presented, which extends the principals of mapping compression patterns to motion patterns and infering the relationship between muscle activity and large tongue motions using tagged cine-MRI. Finally, patient data show considerable asymmetry and unusual motion patterns reflecting the resected anatomy and compensatory strategies used to improve speech production.

The goal of this conference is to learn and study tongue behavior in normal and glossectomy speech. It is worthwhile, therefore, to be aware of the differences between the tongue and most other structures in the human body. The tongue is one of a group of structures known as muscular hydrostats (Kier and Smith 1984, Smith and kier, 1989). Muscular hydrostats, such as tentacles, tongues and the elephant's trunk, are structures that are composed entirely of soft tissue: muscles, fat, connective tissue. They are capable of a rich combination of shapes and motions because of the interaction of orthogonal muscle architecture and an incompressible structure. The incompressibility means that expansion and compression must trade off so that when deforming a three-dimensional structure like the tongue, at least one plane must stretch in opposition to the other two. Compression or expansion in all three directions would indicate a compressible body.

Because of the complex muscle architecture of the tongue, determining its muscle activation patterns is a challenge. Electromyography (EMG) has been used to study muscle activity in the tongue, however, the data are confounded by the interdigitated muscles, such as Transversus and Verticalis (Takemoto). Tagged-Cine MRI (tMRI) augments EMG. tMRI tracks tissue points within the structure of interest and allows calculation of local tissue strain (i.e., stretch), displacement and velocity. Nevertheless, tMRI cannot measure activation of specific muscles in the way that accurately placed fine-wire EMG electrodes can.
Although tMRI does not capture muscle contraction, the direction of fiber compression is accurately determined, so orthogonally positioned fibers, like Transversus and Verticalis are completely differentiated. Analysis of orthogonal planes of a muscular hydrostat reveal specific areas of compression and expansion that can be linked to muscle anatomy. This can be seen clearly in the section below examining lip behavior.

LIPS

The lips are muscular hydrostats with fewer degrees of freedom than the tongue. The combined use of high-resolution MRI and tagged cine-MRI compare location and direction of muscles with related strain patterns. High-resolution MRI (h-MRI) optimizes the combination of coils, field-of-view and slice thickness to improve spatial resolution of human tissue. Murano and Honda (2005) used hMRI to study lip muscles. A TMJ coil was placed close to and parallel

to the surface of the lips of a male, Japanese speaker. A total of 26 slices of 2mm thickness, using a field-of-view (FOV) of 64mm, yielded MR images with a resolution of 0.125mm/pixel. This resolution made it possible to localize muscle and other labial structures in detail as shown in Fig. 1. The orbicularis oris (OO), mentalis (M) and depressor labii inferioris (DLI) muscles were visualized (see Fig. 3 for more details), delineated and reconstructed into 3-dimensional images (Murano and Honda, 2005).

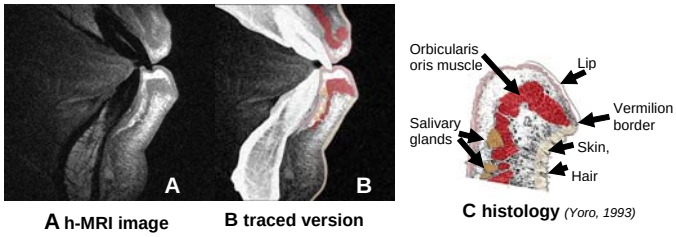

Fig. 1. (A) Midsagittal hMRI image of the lips was (B) hand-traced, and colored, showing (C) structures that were identified in histological slices. [from Murano and Honda 2005].

Data from tagged-cine-MRI (tMRI) is complementary to that of high-resolution MRI (h-MRI). Although tMRI cannot tell us whether muscle compression is due to active contraction, the registration of principal strains (strains in the principal direction) and muscle bundle directions can provide support for hypotheses involving muscle activity. A t-MRI sequence was obtained from the same subject described above, pronouncing the utterance /iu/. A total of 12 time-frames were acquired in 667ms (with a frame duration of 55.6ms) to represent the syllable. The motion from /i/ to /u/ began at time-frame 4 and maximum /u/ was reached at time-frame 9 Ten sagittal, 13 coronal and 11 axial slices (5 mm thick, field-of-view 200mm) were obtained, yielding tagged images with a resolution of approximately 1.6 mm/pixel.

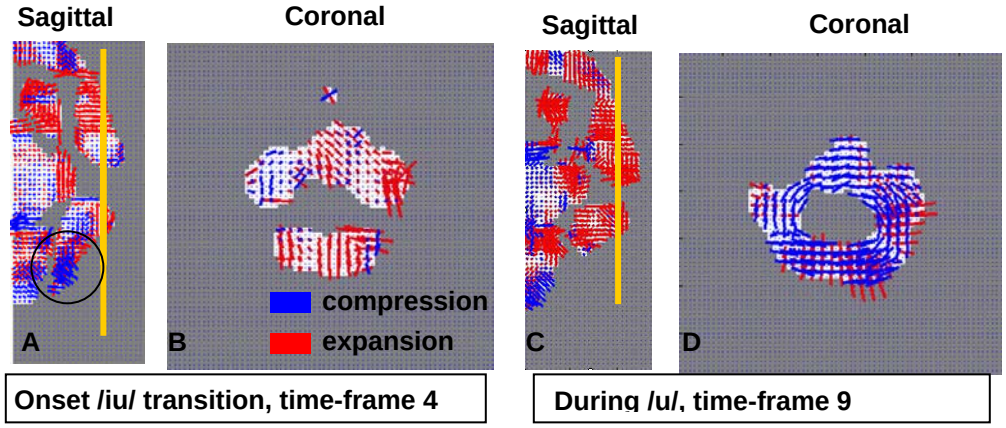

Fig. 2 t-MRI during transition of /i/ to /u in sagittal and coronal views (A and B) and 278ms later during /u/ production for the same sagittal and coronal slices (C and D).

Of great interest in this data set is that the timing of muscle compression is visible in the sequence. Figure 2A and B show the upper and lower lips in sagittal (A) and coronal (B) views at the onset of the motion of between /i/ and /u/ in time-frame 4. In the sagittal view (A) there is an area (in the black circle) that shows increased compression (blue) just below the lower lip, but the lips themselves show relatively little or no strain. The coronal slice (B) from the same time-frame (represented by the yellow line in the sagittal view) shows relatively low levels of strain as well (indicated by the density of the colored lines). Examination of labial tissue behavior in both planes is important, because the lips are also considered to be a muscular hydrostat system, where volume is preserved and muscles are interdigitated and run in different directions (Blair 1986). The analysis of the same sagittal and coronal slices 278ms later, in time-frame 9 (Fig. 2C and D respectively) shows a different pattern. There is an evident labial protrusion and a large amount of expansion (area of dense red lines) in the sagittal view (C) and an increased pattern of compression (dense blue lines) in the coronal view (D). As described below, the interpretation of

the compression and expansion patterns was aided by comparing these findings with h-MRI images of the same subject for static positioning during /u/.

Fig. 3 shows h-MRI images of the same subject. These data are very useful for showing muscle architecture, especially because they can be acquired in thin slices (2mm in this case). The fiber bundle directions of mentalis and depressor labii inferioris muscles are clearly evident as striations in Fig. 3A and B. To interpret t-MRI strain patterns in relation to possible muscle activity, the planes of h-MRI and t-MRI slices should be identical. In this case, however, the slices are not identical. Therefore we matched the two adjacent 2mm-thick h-MRI slices with the single 5mm t-MRI slices that contains them both.

The direction of compression of the blue principal strain lines encircled in Fig. 2A is the same as those of the mentalis muscle (Fig. 3A) and not the depressor labii inferior (Fig. 3B). Although principal strains should not be interpreted as equivalent to muscle contraction, it is apparent that the predominance of compressive tissue displacement is in the same direction as expected from contraction of the mentalis muscle.

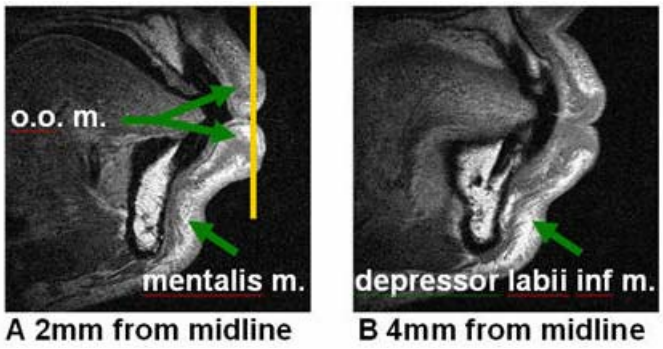

Fig. 3 Sagittal hMRI of lips during static /u/. (A) Arrows show mentalis, orbicularis oris superior and inferior. (B) Arrow shows depressor labii inferior. The yellow line is the coronal slice in Fig 2.

Such observations make it possible to more accurately identify the muscles that are engaged in the two-stage activation sequence for lip protrusion for /u/, as observed above. In Fig. 2A mentalis muscle can now be associated with the area of compression below the lower lip, which occurs before the compression of the orbicularis oris, shown in Fig. 2D. The timing difference between the compression of mentalis and orbicularis oris leads to the inference that the protrusion observed for the vowel /u/ involves a sequencing of activations of the two muscles (Murano, et al, 2005).

TONGUE

The complicated, anisotropic motions of the tongue can be explored using principal strains and velocity fields derived from tMRI data sets. These measurements are exploited to determine the relationships between different tongue regions during speech. Principal strains show direction of local tissue compression. Velocity fields show direction of tissue point motion between two fields. The motion may be due to stretch or to translation. Separate measures of stretch and translation are very important in muscular-hydrostat motion because they allow estimation of possible muscle activity (compression) as distinct from the resulting motion

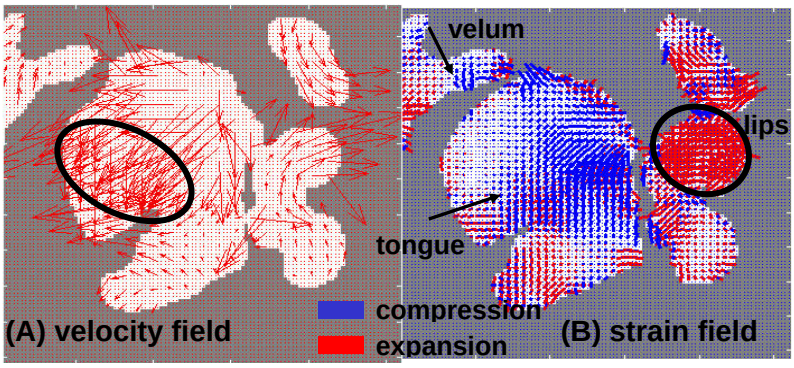

Figure 4: Tagged Cine-MRI data for time-frame 4-5. Velocity fields (left) indicate direction of motion of local region of the tongue and lips. Lips on right. Principal strains (right) show local compression (blue) and expansion (red).

(translation). Figure 4 shows velocity fields (A) and principal strains (B) for the beginning of the transition from /i/ to /u/ (subject is a male Tamil speaker). Longer velocity lines indicate more rapid motion and longer strain lines indicate greater compression or extension. Figure 4B shows lip expansion (circled) consistent with compression in the Orbicularis Oris direction (cf. Figure 2D). The result of this expansion is forward motion of the lips (Figure 4A). On the other hand, the backward motion of the posterior tongue (oval) is not accompanied by local stretch (Figure 4B). Instead compression occurs in the anterior tongue. Thus the posterior tongue appears to move as a rigid body. This analysis was performed in the sagittal plane only.

An important principle of muscular hydrostat deformation is incompressibility, that is, strain in one plane is accompanied by oppositional strain in at least one other plane (Parthasarathy et al., 2007). Analysis of all three orthogonal planes is necessary to understand how such tongue deformations are accomplished. This principal is visible on tMRI data. The tongue motion from /u/ to /k/ requires upward and forward motion of the tongue body so that the upper surface contacts the palate in the appropriate position for /k/. In order to elevate this region, translation and stretch occur.

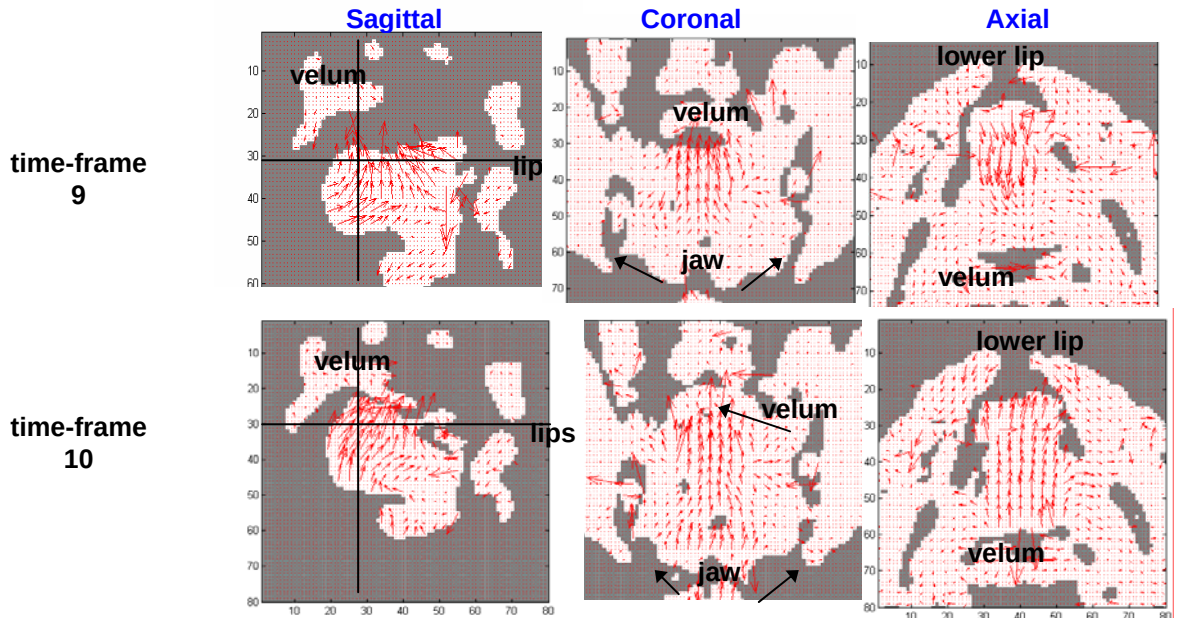

Figure 5 Velocity fields show direction of early (top) and late (bottom) motion from /u/ to /k/ in the midsagittal (left), coronal (middle), and axial (right) planes. Longer arrows indicate faster motion. Black lines indicate location of coronal and axial slices.

Figure 5 shows velocity fields for a three-plane data set, taken from the utterance /disuk/, during the transition from /u/ (tf 9 - top) to /k/ (tf 10 - bottom). The complete data set consists of 8 sagittal, 9 coronal and 9 axial slices, 5 mm thick with a 2 mm interslice gap in the coronal and axial planes. For each slice 12 time-frames were collected. The motion into /k/ requires maximal elevation of the tongue as it must form a firm complete contact with the palatal vault and lateral margins. In the presented subject the tongue body for /u/ is fairly low, so that the tongue must move considerably into the /k/. The /k/ occurs at time-frame (tf) 10. The velocity fields for all three planes reflect the large motion of the tongue body. In the midsagittal slice (top) the velocity fields reflect the upward motion of the tongue body toward the palate. The motion is not purely vertical, however, initially (tf 9) it converges from all regions of the tongue towards the part that will make contact with the palate. As the tongue reaches maximum (tf10), the motion is more uniform and contains some forward motion. The coronal data (Figure 5, column 2) indicates that the upward motion of the tongue (tf9) is followed by upward motion of the floor of the mouth (tf10). Finally the axial data shows a rapid switch in direction from backward (tf9) to forward (tf10), reflecting coarticulation. In tf 9 the anterior tongue moves back. The other slices tell us that the posterior tongue moves up. In

the maximal /k/ (10) the tongue is already sliding forward in preparation for the next repetition of the work and the onset of /d/. The velocity fields clarify the complex 3D motion needed for such a large elevation.

Tissue point motion, however, does not tell whether stretch or translation effected the movement. Examination of principal strains the three directions reveals considerable involvement of the tongue muscles to execute this extreme upward propulsion. Figure 6 shows low resolution magnitude images from cine-MRI, at time-frame 9, for orientation of the principal strains. The principal strains from tf's 9 and10 ar shown in the middle and bottom rows respectively. The tissue slices, from left to right, are lateral sagittal, posterior coronal, anterior coronal, superior axial.

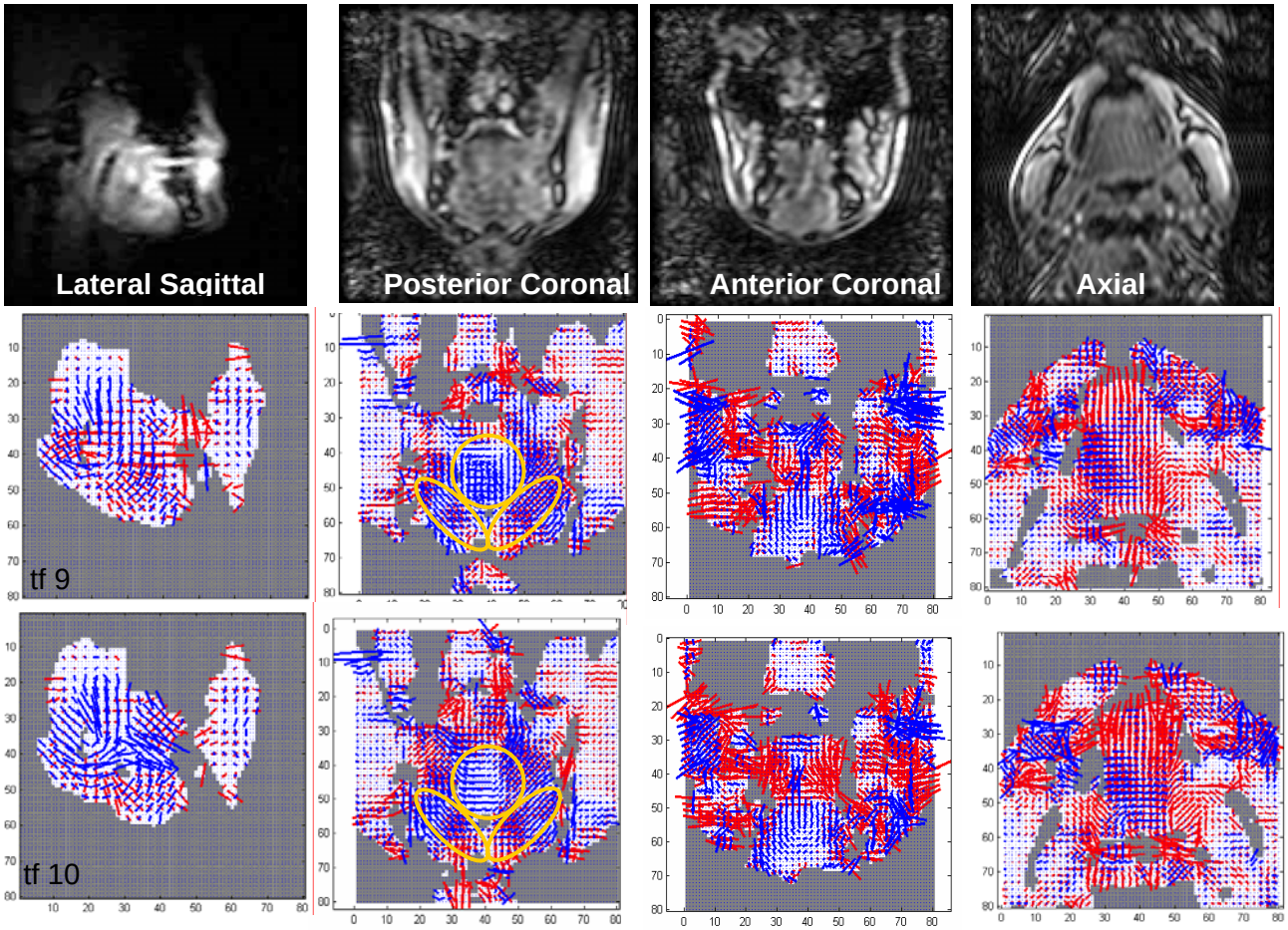

Figure 6 Principal strains during transition (top) from /u/ to maximal /k/ (middle), and magnitude image (bottom) for lateral sagittal (left), posterior coronal (3), anterior coronal (6), upper axial (the anterior coronal tongue (slice 3).

We realize that the actual muscle activity cannot be determined from principal strains. From the principal strains we speculate on possible muscle activity based on the patterns of compression. However, the coronal slices are so consistent with muscle fiber directions that we offer speculations about possible muscle activity. Posterior coronal data (column 2) shows a dramatic change between the transition (tf 9) and the /k/ closure (tf 10). At tf 9, simultaneous vertical and horizontal compression is consistent with genioglossus (GG) and transverse (T) activity (yellow circle). In the base of the tongue compression reflects the line of action of mylohyoid (MH) (yellow ovals). One time-frame later the vertical compression is released and the horizontal and oblique compressions rapidly elevate the tongue body (Fig 5 and 6, col 2). The anterior coronal slice also

reveals midline compression consistent with the use of GG. This compression decreases between tf 9 and tf 10. The vertical expansion (oblique red lines) lateral to GG are also consistent with activity in T.

GLOSSECTOMY

A single female patient was seen 8 months after partial glossectomy with tongue tip preservation for a right, lateral, T1N0M0 oral tongue squamous cell carcinoma. The expected pattern of tongue motion for glossectomy speakers is left-to-right asymmetry. Asymmetry results from resected tissue and scar tissue properties, as well as compensatory tongue motion patterns on the contralateral side. Figure 7 shows high resolution static images of the tongue anatomy of the patient, which make visible the scar and asymmetrical surface posture. Figure 7A shows the resected regions and loss of muscles such as inferior longitudinalis (IL), and some intrinsic musculature (T, V). Figure 7B shows the normal left side with intact muscles. Figure 7C shows postural asymmetry in the coronal plane and scar/loss of tissue (circled). Fig 7 C shows resected tissue appears to include IL, T, V, and hyoglossus (HG). Figure 7d shows the AP length of the scar and resected tissue. Yellow lines mark the axial, coronal and sagittal planes discussed in the subsequent data. These images are 3 mm thick and aligned with the tagged images, which are 6 mm thick.

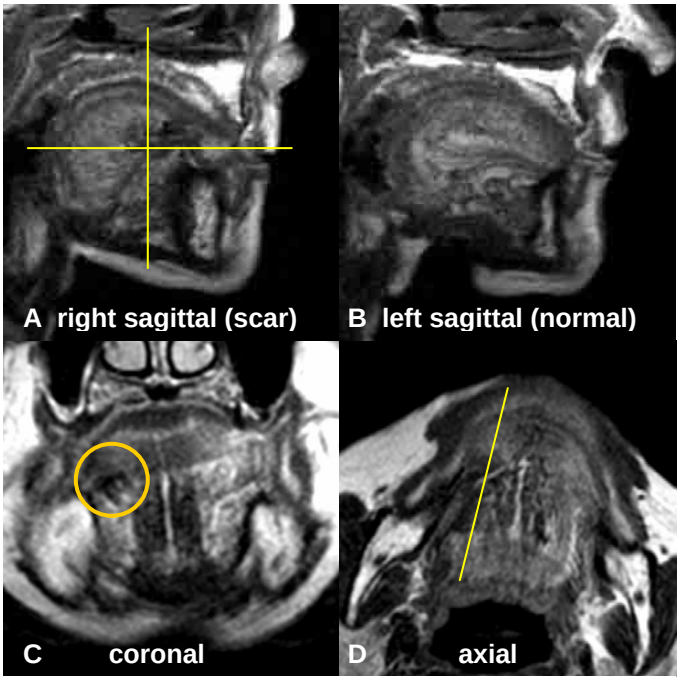

Figure 7. High resolution images of the tongue in the (A) sagittal, (B) coronal and (C) axial planes) show the scar (arrows) in the right tongue. All data shown for this subject is in these planes.

Figure 8 shows two time-frames from a cine sequence of low resolution images of the same subject, as the tongue moves from /i/ (as in 'bee') to /n/ (as in 'new'), taken from the utterance /dzinu/. The coronal tissue slice is depicted in Figure 7A (vertical yellow line). The images show asymmetrical tongue position, with palate contact and lowering on the left (preserved) side. The /i/ has more medial tongue palate contact. The mechanics of this motion are explored in the velocity fields calculated from the accompanying tMRI data. The control of the motion is hypothesized from these and the compression patterns seen in the principal strains.

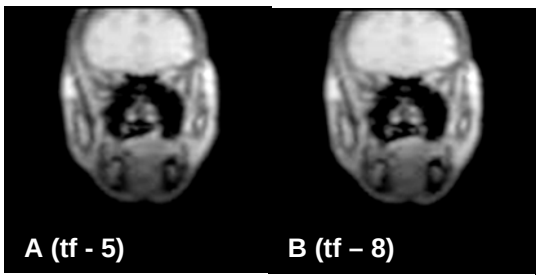

Figure 8. Coronal images show left palate contact (A) and lowering (B).

Velocity fields are presented from three orthogonal planes of data at the moment of peak velocity into the /n/ (see Figure 9). Principal strains for the coronal slice are also shown to further explore the primary direction of motion, which is downward. All slices intersect the scar (see Figure 7). The vectors in the sagittal slice (A) indicate that tongue tip elevation needed for /n/ is executed as part of a front-to-back rotation around the scar (represented as a vortex). The coronal slice (B) is taken fairly far back in the mouth, where the tongue body is in the palatal vault (see Figure 7). The left

tongue starts higher and lowers primarily on the left side, contralateral to the scar. The axial slice (C) shows a little rotation on the left, but motion is small as this slice intersects the scar and the motion here is primarily in the superior or inferior direction (see sagittal data). Of particular interest is the pattern of sagittal rotation used to facilitate tongue tip elevation. The tongue tip is considered to move independently from the body (see Mermelstein, 1973 for earliest representations). In the glossectomy data, tip elevation does not appear to be an independent degree of freedom, but rather, the mechanism for tip elevation involves front-to-back rotation of the entire tongue, in which the tip is carried upward. This motion pattern has not been seen previously in normal subjects.

The principal strains (Figure 9(D)) show that the strategy for tongue lowering motion is vertical compression contralateral to and below the tumor, with multidirectional expansion at the tumor location. The expansion is consistent with the tumor being passively pulled downward and toward midline in response to the surrounding compression.

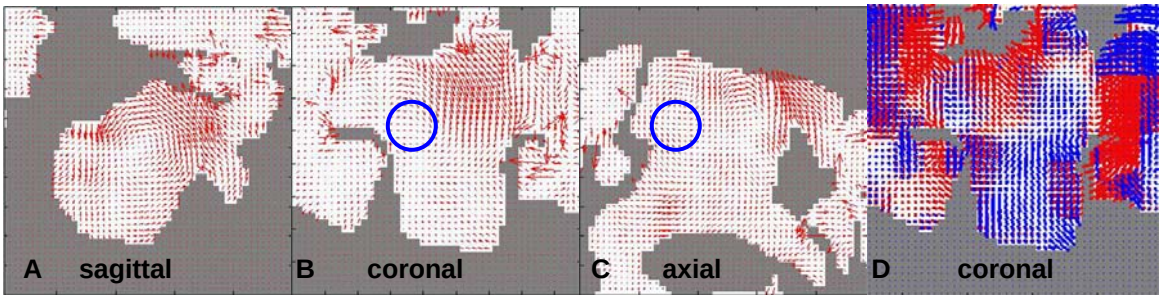

Figure 9. Time-frame 5 shows motion from /i/ to /n/ includes (A) backward rotation to elevate the tip, (B) lowering on the left side only and (C) little AP motion.

Velocity fields taken from the time-frame of peak velocity from /n/ into /u/ (120 ms later) reveal a very different pattern of motion (see Figure 10), as the earlier rotation pattern resolves into a more linear backward motion in the upper tongue. Figure 10 shows directly backward motion for the upper tongue in the sagittal (A) and axial (C) planes. In the axial plane (C) the left tip is has moved farther back and its motion is faster. The coronal plane (B) shows rotation in which the unaffected side moves upward and the resected side lowers. Thus, the mechanism for backward displacement includes counterclockwise rotation in the coronal plane. However, the scar is not a vortex, rather the intact left side elevates and the scar tissue lowers. Figure 10 (D) shows the principal strains in the axial direction, the primary direction of tongue motion from /n/ to /u/. The

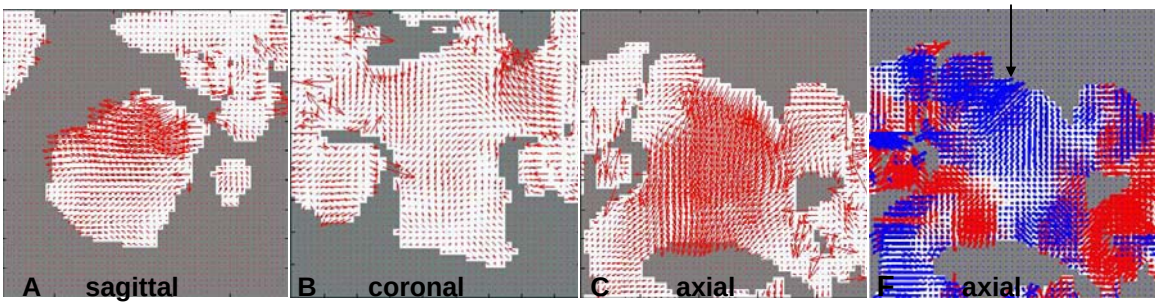

Figure 11. At time-frame 8 velocities show motion from /n/ to /u/ is primarily backward in the upper tongue (A) (C). Vertically the tongue rotates from left to right counterclockwise (B). Principal strains show vertical compression primarily and oblique tip compression anterior to the scar.

strains show primarily backward compression with a small region of oblique compression on the right, anterior to the scar (arrow). This region is the preserved tip.

We hypothesize several factors that could create this unusual pattern. The first is that the rigidity of the scar creates difficulties for tongue tip elevation. The second is that the neurological control of the preserved tip is reduced by the loss of the resected tissue, creating aberrant muscle contractions. Third, muscles, such as transverse or verticalis, may be attached to the scar in a more AP fiber orientation resulting in an oblique compression pattern in the tip.

CONCLUSIONS

The combination of high resolution MRI and tagged cine-MRI create a powerful method for testing hypothesis about motion patterns and deformation strategies required to move the tongue and lips during speech. Muscle fiber location and direction can be discerned from hMRI images. Compresion in the direction of specific muscles appear in principal strain maps. These can be combined with velocity fields to estimate how tongue deformation emerges from the relationships between muscle directions and local compression. Three-dimensional data allows local patterns of motion and compression to be isolated and better compared to muscle anatomy. This method applies very well to the aberrant deformations seen in glossectomy speakers. Here we presented one example of partial glossectomy with tip preservation and no flap reconstruction. The patient data shows compensatory mechanisms of motion that include rotational and asymmetric motions to execute large displacements. Direction of rotation varies depending on the motion being executed (elevation vs. backing). Compensatory patterns can be directly related to changes in oral morphology such as scar tissue, and residual tip tissue. Subsequent work needs to provide additional detail on glossectomy strategies and their relationship to tissue loss and surgical reconstruction.

References

Blair, C. (1986). "Interdigitating muscle fibers throughout orbicularis oris inferior: preliminary observations." J Speech Hear Res, 29(2), 266-9.

Kier W, and Smith K, 1984, (1985) Tongues,tentacles, and trunks: The biomechanics of movement in muscular-hydrostats. *Zoological Journal of the Linnaean Society*, **83**, 307-324.

Mermelstein, P (1973) Articulatory model for the study of speech production. *Journal of the Acoustical Society of America*, **53,** 1070-1080.

Murano, E., and Honda, K. (2005). "Mechanism of lip protrusion in vowel production." Tech Rep IEICE, SP2004-140, 19-24.

Murano EZ, Stone ML, Honda K. Muscular Hydrostat mechanism for lip protrusion in speech. *Acoustical Society of America*, Minneapolis - USA, October 2005.

Parthasarathy, V., Stone, M., NessAiver, M., and Prince, J. L. (2007) Understanding tongue motion from tagged magnetic resonance images using harmonic phase MRI. *Journal of the Acoustical Society of America,* **106**, 2974-2982.

Smith, K.K. & Kier, W.M., (1989) Trunks, tongues and tentacles: moving with skeletons of muscle, *American Scientist*, **77,** 29-35.

Takemoto, H. (2001). "Morphological analyses of the human tongue musculature for three-dimensional modeling." J Speech Lang Hear Res, 44(1), 95-107.